PHYSICAL REVIEW B VOLUME 56, NUMBER 1 1 JULY 1997-I

ARTICLES

Soliton dynamics in a type-II incommensurate-commensurate system: Betaine calcium chloride dihydrate (BCCD)

M. le Maire, R. Straub, and G. Schaack
Physikalisches Institut der Universität Würzburg, Am Hubland, D-97074 Würzburg, Federal Republic of Germany
(Received 6 January 1997)

The results of dielectric experiments on pure and Br-doped betaine calcium chloride dihydrate (BCCD) at variable temperatures T, hydrostatic pressures p, and quasistatic electric fields E are presented, which show the occurrence of field-induced commensurate (c) phases proving the existence of a square-wave modulated polarization at low T. With increasing T the shape of the modulation wave turns rather smoothly into an almost harmonic wave in the incommensurate (ic) region. Near the transition temperature c($\delta=\frac{1}{4}$)$\rightarrow$ic at $T_{1/4}$ indications for the onset of a gliding polarization wave (phason) in the ic phase, but also in the narrow c phases above $T_{1/4}$ with an almost harmonic modulation were detected in BCCD. This range extends up to T_i. [S0163-1829(97)00725-X]

I. INTRODUCTION

Spontaneously formed superstructures in condensed matter are encountered, e.g., as soliton lattices in commensurate (c) and incommensurate (ic) modulated crystalline phases,[1,2] in charge-density waves[3] and in the vortex lattices of magnetic-flux lines in superconductors.[4]

Like domain walls solitons separate almost commensurate regions (c domains) of width d. In ic-c systems with an Ising-like modulation (square wave at low temperatures T) the soliton pattern is regular, separating microdomains which have a size of a few lattice constants a_0 of the high-T parent (p) phase, and is — in the simplest case — determined by competing nearest- and next-nearest-neighbor interactions.[5,6] Solitons interact with each other (usually repelling). In ferroelectrics their width b at low T is generally of the order of a_0 (soliton density $n=b/d\ll 1$) and increases toward d near T_i ($n=1$), where the phase transition p$\leftrightarrow$ic occurs.[7–9]

As a consequence the modulation just below T_i is sinusoidal and the soliton concept is no longer valid. Models of ic systems in terms of Landau theory can be roughly divided in two classes (I and II), according to whether the term in the free-energy density responsible for the appearance of the ic phase is linear (I) or quadratic (II) in the gradient of the order parameter P (whether it includes the Lifshitz invariant or not). Systems with a c phase at low T, i.e., when the soft mode of the system finally condenses at a finite wave vector $\mathbf{q}$ (e.g., in the A_2BX_4 compounds), belong to class I with a two-dimensional order parameter, while an unmodulated, ferroelectric (f) low-temperature phase (as in BCCD, thiourea, and $NaNO_2$, where the soft mode condenses at $|\mathbf{q}|=0$ and the order parameter is one-dimensional) indicates a type-II classification.[2]

The evolution of the modulated phases from the p phase in type-I compounds is well documented both by experiments and Landau mean-field theory:[1,2] below T_i the modulation is sinusoidal, whereas near the lock-in transition ic $\rightarrow$c at T_c it becomes solitonlike, i.e., periodic regions with approximately a constant phase of the modulation (the phase between the unmodulated periodic lattice structure and the superstructure) are separated by solitons (= discommensurations), where the modulation phase varies rapidly to the next constant (c) value. Below T_c the modulation is mostly square wave.

In type-II compounds the situation is less clear: the range of discommensurations is reduced to a very narrow T interval above T_c, the modulation in the c phases has been traced to be either harmonic or anharmonic to square wave. In $NaNO_2$, where the modulated phase is only $\Delta T=1.5$ K wide, i.e., the system is close to the multicritical Lifshitz point, the modulation is found to be harmonic. In thiourea ($\Delta T=33$ K) a coexistence of solitonic and sinusoidal structural modulation of different parameters has been observed and explained.[10] The results in BCCD are still contradictory.[11–13] Here $\Delta T=118$ K, the system is far from the Lifshitz point and appears to be intermediate between types I and II.

In this paper we present results for pure and Br-doped BCCD from dielectric experiments under hydrostatic pressure p and quasistatic high electric fields E, which demonstrate a continuous evolution of the modulation of the polarization (order parameter) from sinusoidal at T_i (164 K) via various c phases[14] to a square-wave modulation at low T. The modulation period $\tilde{p}$ increases on cooling, ending in a f phase ($|\mathbf{q}|=0$). The modulation amplitude varies rather smoothly at the different c-c transitions. Thus, in BCCD the modulation appears to follow a scenario different from behaviors of both types I or II.

II. EXPERIMENTS

BCCD, $(CH_3)_3NCH_2COO\cdot CaCl_2\cdot 2H_2O$, $Z=4$ is well known for its incomplete and harmless devil's staircase behavior[14] with many c phases developed according to the

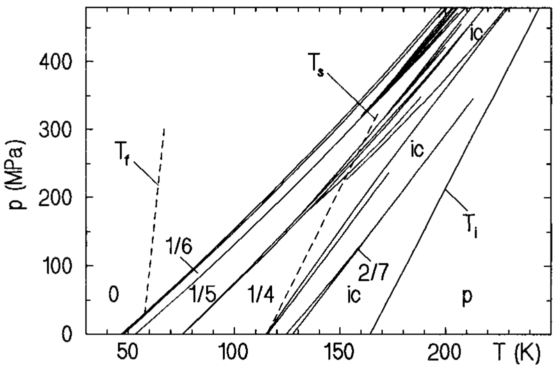

FIG. 1. (p,T)-phase diagram of BCCD; the parent (p) and some major incommensurate (ic) and commensurate phases ($\delta = n/m$) are indicated. The dielectric anomalies T_f and T_s are discussed below.

Farey tree law,[15] demonstrating under the application of hydrostatic pressure c structure branching processes and their accumulations (Fig. 1).[9,16] The spontaneous polarization P_s in the f low-temperature phase is along the b axis, the modulation axis is along c $[\mathbf{q} = \delta(T,p,E)\cdot \mathbf{c}^*]$.[14] In Br- and Mn-doped BCCD ($BCC_{1-x}B_xD$, Br^- substituting Cl^-, and $BC_{1-x}M_xCD$, Mn^{2+} substituting Ca^{2+}, respectively) and also in γ-irradiated BCCD the number of observed c phases is reduced, and a strong increase of the thermal hysteresis as well as a widening of the ic region at the expense of the c region are encountered.[17–19]

We have observed the hysteresis loops of pure and Br-doped BCCD ($x = 0.02$, 0.08) with $E \lesssim 40$ kV/cm, $0.1\ \text{Hz} \leqslant \nu \leqslant 100$ Hz applied along b, varying p with helium gas for pressure transmission and T. P_s values of spontaneous and field-induced polar phases have been measured and the $(E_b, T; p)$ diagrams have been determined. Some results are shown in Fig. 2. The polar phases ($\delta = \frac{2}{11}, \frac{2}{9}, \frac{2}{7}$) grow with

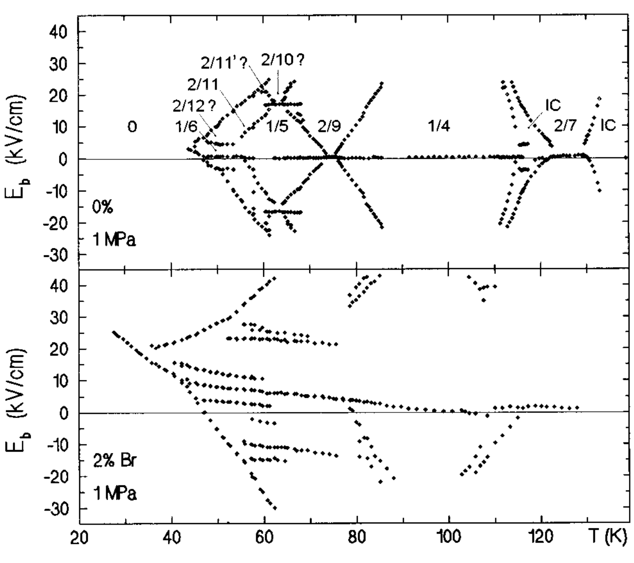

FIG. 2. Electric field vs temperature (E_b, T) diagrams of pure and 2%Br-doped BCCD (more (E_b, T) diagrams of pure BCCD can be found in Refs. 13, Fig. 1 and 19, Fig. 6.46). A small hydrostatic pressure ($\approx$ 1 MPa) has been applied to protect the sample against electrical discharges at high fields.

E_b at the expense of nonpolar phases ($\delta = \frac{1}{5}$) or of the a-polarized improper phases ($\delta = \frac{1}{4}, \frac{1}{6}$) with an E dependence linear for c-c and nonlinear for c-ic transitions.[20] Surprisingly, the slopes dT_c/dE are approximately equal for all transitions, with growing T these slopes are slowly decreasing. At high fields the nonpolar phases [e.g., $\frac{1}{5}$, $\frac{1}{6}$, $\frac{1}{4}$ (extrapolated)] cease to exist and give rise to field-induced phases, the phase boundaries of finite length have zero slopes, ending in two triple points. These field-induced phases also exist in crystals doped with impurities (Fig. 2), where the higher-order c phases are suppressed[18] (measurements on Mn-doped BCCD with $x = 0.05$ essentially lead to the same results;[19] the bending of the diagrams in Fig. 2 at low T away from $E = 0$ is due to the coercive field, growing with decreasing T and with the impurity concentration).

The P_s values of the polar phases $\delta = n/m$ (n even, m odd) (Ref. 14) are found to be equal to $P_{s,0}/m$ within the experimental errors of a few percent [T effects considered; $P_{s,0}$ is the value found for the unmodulated f phase ($\delta = 0$) at low T, $P_{s,0} = 2.4\ \mu\text{C/cm}^2$ (Ref. 21)]. The P_s values of the field-induced phases are found to be the sum of the P_s values of the two neighboring polar phases [e.g., $P_s(\delta = \frac{2}{10}?) = P_s(\delta = \frac{2}{9}) + P_s(\delta = \frac{2}{11})$].[13] Comparing our results for P_s with values from other experiments (e.g., from pyroelectric measurements,[22]) one has to take into account that our samples are subject to high electric fields, which eliminate domain-wall effects and the influence of impurity pinning on P_s.

This result demonstrates the validity of the model of the Ising-type modulation in BCCD: The polarization in adjacent microdomains is antiparallel, P_s of a c phase results as the sum over at least two such domains. Thus $P_s(\delta = \frac{2}{9}) = P_{s,0}/9$, because the contribution of one out of nine dipole layers [in the context of the ANNNI (axial next nearest neighbor Ising) model[7–9]] is not compensated: $\langle 45\rangle \equiv \uparrow\uparrow\uparrow\uparrow\downarrow\downarrow\downarrow\downarrow\downarrow$ (here: period $\tilde{p} = 9$), where each arrow represents one dipole layer oriented perpendicularly to the modulation vector $\mathbf{q}$. To be correct, our model requires polarization saturation in each pseudospin layer (low T) and $b \ll m a_0$ (square-wave modulation). The P_s values of the field-induced phases result from the spin flip of one layer per period $\tilde{p}$, e.g. $\langle 6\rangle \to \langle 57\rangle$, $\langle 56\rangle \to \langle 47\rangle$,[24] i.e., the collective shift of every second soliton by a_0, while $\tilde{p} = \text{const}$. Such a phase transition has, to our knowledge, not been observed previously.

We have also studied in detail two dielectric anomalies (T_s, T_f) found in pure, Br-doped ($x \lesssim 0.08$), Mn-doped ($x \lesssim 0.05$) and γ-irradiated BCCD (doses $\lesssim 20$ kGy) (Refs. 17 and 19) at low field strengths and frequencies $200\ \text{Hz} \leqslant \nu \leqslant 2$ MHz, which differ from the anomalies at the usual c-c or ic-c phase transitions: In the real part of the dielectric constant, $\varepsilon'(T)$, both anomalies are broader and less pronounced than those at structural phase transitions, whereas the dielectric loss, $\tan\delta(T) = \varepsilon''/\varepsilon'$, displays marked maxima at T_s and T_f. They are more pronounced in doped and γ-irradiated BCCD than in nominally pure BCCD, where they are observed only at elevated pressure. In Fig. 3 we have plotted the weak frequency dependences of the shapes of the anomalies T_s and T_f [both depend on pressure (Fig. 1) and concentration (Fig. 4 and Ref. 18, respectively].

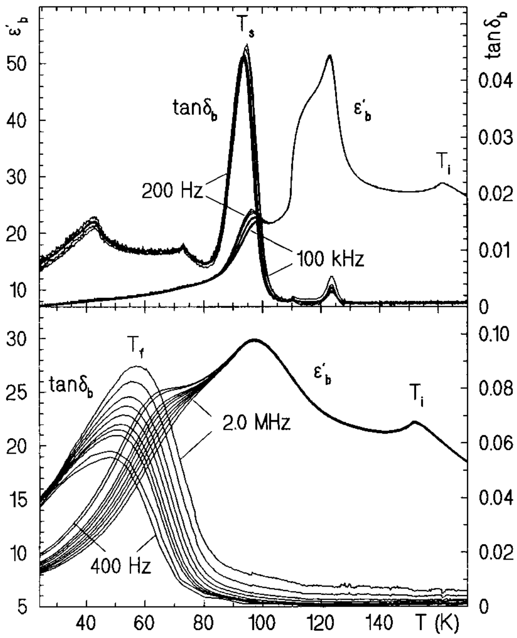

FIG. 3. Dielectric anomalies T_s and T_f in Br-doped BCCD. Above: $\varepsilon'_b(T)$ and $\tan_b\delta(T)$ of $BCC_{0.98}B_{0.02}D$ at various frequencies (ambient pressure, $\dot{T}>0$) Below: $\varepsilon'_b(T)$ and $\tan_b\delta(T)$ of $BCC_{0.92}B_{0.08}D$ at various frequencies (ambient pressure, $\dot{T}>0$).

T_s and T_f have been observed previously, T_s also by other groups,[21,25,26] but have not been interpreted.

III. DISCUSSION

Information on the T-dependent soliton width b can be obtained applying the Clausius-Clapeyron equation

$$dT_c/dE = -\Delta P/\Delta S \tag{3.1}$$

to the (E,T) diagrams of Fig. 2, where ΔP is known from the polarization measurements, and ΔS can be determined and compared with a simple model calculation of the transition entropies: We interpret a soliton by a single, isolated layer of pseudospins, which is completely disordered. When a soliton is formed, the entropy changes: $\Delta S_M = N_s k_B \ln 2$ (N_s: number of pseudospins within a soliton per mole: $N_s = N_p f_s$ with N_p: number of pseudospins per mole, $N_p = 3.011\times 10^{23}\,\mathrm{mol}^{-1}$ [two spins per cell[23]) and f_s: soliton density $(=\delta)$]. Thus at the c_1-c_2 phase transition $\Delta S_M = N_p k_B \ln 2\cdot(\delta_2-\delta_1)$.

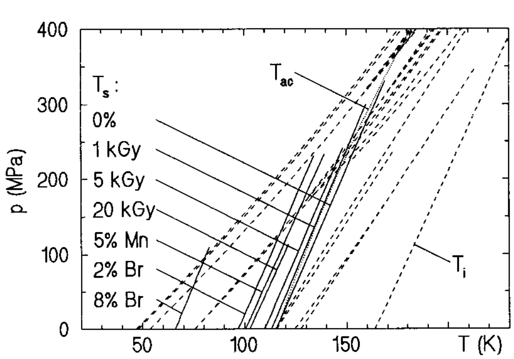

FIG. 4. Position of the T_s anomaly for various impurity concentrations and γ-irradiation doses (in kGy) with respect to the (p,T)-phase diagram (broken lines) of pure BCCD. The accumulation line T_{ac} is also shown as dotted line.

TABLE I. Entropy changes ΔS at various phase transitions in BCCD in J/mol K from specific heat (ΔS_H) (Ref. 27), from Eq. (3.1) (ΔS_C), and from the soliton model (ΔS_M).

Phase transition	ΔS_H (Specific heat)	ΔS_C From Eq. (3.1)	ΔS_M (Soliton model)
$f\leftrightarrow\frac{1}{6}$	Not measured	0.572	0.4800
$\frac{1}{6}\leftrightarrow\frac{1}{5}$	0.11	0.114	0.0959
$\frac{1}{5}\leftrightarrow\frac{1}{4}$	0.16	0.149	0.1440
$\frac{1}{4}\leftrightarrow$ ic	0.05	0.043	}0.1028
ic$\leftrightarrow\frac{2}{7}\leftrightarrow$ic	0.01	0.032	

In Table I we have compiled values of the entropy changes as determined from the observed specific-heat anomalies,[27] from Eq. (3.1), and from the above model. We find the agreement surprisingly good. It can be improved, if b is increased slightly beyond a single layer. At higher T (ic $\leftrightarrow\frac{2}{7}$), ΔS_M is larger than the experimental value, because the modulation is nearly harmonic and P_s is clearly below $P_{s,0}$, i.e., the entropy increase on creating a new soliton is smaller than anticipated from the model. At low and intermediate T, ΔS_C increases with T for long-$\tilde{p}$ phases (Fig. 5) because of the increase of b, the modulation is still anharmonic, but is approaching the case of a harmonic modulation. A model of the T-dependent soliton shape and overlap is beyond the scope of this paper.

Additional information on the solitons can be derived from the field-induced phases. They indicate a constant soliton density at these transitions ($\Delta S=0$), however one soliton sublattice is shifted by a_0, e.g., $\langle 5\rangle\rightarrow\langle 46\rangle$ away from the position which minimizes the repulsive interaction. The phases are not on the Farey tree. An increase ΔF of the free-energy results, which is compensated at the critical field E_c of the transition by the polarization energy $\Delta F_E = -E_c\Delta P$, where ΔP is the polarization increase due to the soliton shift. Using the ansatz of an exponential soliton interaction,[28] the total free energy for one soliton in the soliton lattice (modulation period $\tilde{p}$) reads

$$F = [F_s + 4A(e^{-X/b'} + e^{-Y/b'})]/\tilde{p}, \tag{3.2}$$

where X and Y are the soliton distances in units of a_0, $X+Y=\tilde{p}$. A is the soliton formation energy and b' is the

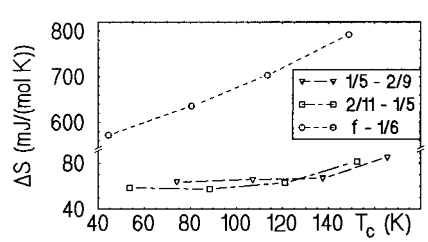

FIG. 5. T (or p)dependence of the entropy change ΔS_C for various c-c transitions.

soliton interaction range. F changes for a soliton shift of a_0 from $\langle m\rangle$ to $\langle m-1,m+1\rangle$ (Ref. 24) by

$$\Delta F=(8A/\widetilde{p})e^{-ma_0/b'}[\cosh(a_0/b')-1]. \qquad (3.3)$$

This free energy will be compensated for the c phase $\langle m\rangle$ by $E_{c,m}\cdot P_{s,0}/m$. As an average over the field-induced phases $\langle 46\rangle$, $\langle 57\rangle$, $\langle 47\rangle$ we determined the soliton range $b'=0.67$ in terms of a_0, and $A=10.6\ \mathrm{Ws/cm^3}$ with an uncertainty of $\pm 20\%$; $E_{c,4}\approx 75$ kV/cm. Both the interaction range $b'\cdot a_0$ and the soliton width a_0 are of comparable size, which demonstrates the consistency of our interpretations.

As a consequence these results indicate that the formation energy of local defects in the modulation pattern of c phases near pinning centers should be low and hence such defects will occur frequently and have to be considered.

IV. THE ANOMALIES T_s AND T_f

The anomalies T_s and T_f, which are both intrinsic features of BCCD, appear to be related to the soliton system for reasons to be discussed in this section. The anomaly at T_f can be interpreted as due to domain freezing because it is closely related to similar, well established phenomena in KDP:[29] Below T_c the mobility of isolated domain walls at high ac fields contributes to the large values of ε' above T_f, while the abrupt ε' drop below T_f indicates their freezing.[30] Figure 3 displays the close relation between the phenomena at T_f and T_s in this respect. It is tempting to interpret the anomaly at T_s as a freezing of the soliton lattice, i.e., above T_s occurs a random, collective shift or glide (depinning) of the solitons with respect to the lattice. The onset of gliding at T_s is accompanied by the formation of local polar defects ($P||b$) of the modulation: e.g., $\langle 4\rangle\rightarrow\langle 35\rangle_{\mathrm{local}}$, $\langle 5\rangle\rightarrow\langle 46\rangle_{\mathrm{local}}$ due to soliton pinning centers. The average modulation period does not change at T_s. Our interpretation of T_s is backed by the following observations or conclusions:

(A) We have studied T_s under hydrostatic pressure.[13] The slopes dT_s/dp are different from those of the c-c transitions but they are parallel for all defect concentrations and parallel to T_i (Figs. 1 and 4). In pure BCCD the line $T_s(p)$ coincides within error limits with a line which connects the accumulation points in the structure branching regions[16] [$T_{\mathrm{ac}}(p)$ in Fig. 4]. This accumulation line separates the incomplete ($T>T_{\mathrm{ac}}$) and harmless ($T<T_{\mathrm{ac}}$) devil's staircase region in BCCD.[13] According to the ANNNI model, ic structures only occur above T_{ac}.[9] In the $\frac{1}{4}$ phase ($\equiv\langle 4\rangle$ phase), lines of constant polarization $P_{s,a}$ also run parallel to T_{ac}. T_s or T_{ac} coincide with a line of 56% ($=14\ \mathrm{nC/cm^2}$) of $P_{s,a}$ at $T=75.5$ K, $p=0.1$ MPa. The T_s anomaly occurs, if the modulation amplitude falls below a certain limit (on heating). Here the modulation wave is nearly harmonic.

(B) T_s strongly depends on the impurity or pinning-center concentration x (Fig. 4). For growing x, T_s decreases, approaches T_f and in Br-doped BCCD the two anomalies finally merge for $x\approx 0.08$ (Fig. 6). This result can be easily interpreted assuming collectively fluctuating solitons and their local pinning at lattice defects: With increasing x the regions of coherent gliding are shrinking and finally the small unpinned soliton sections are fluctuating incoherently

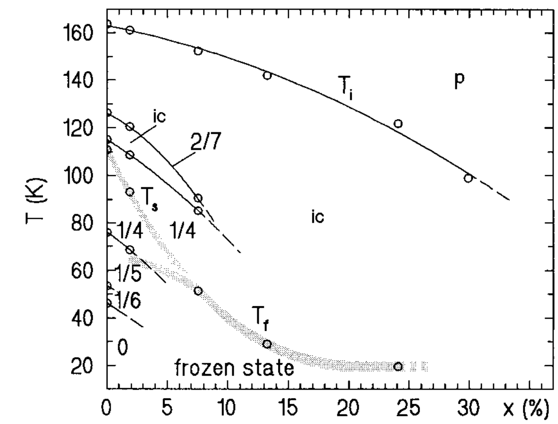

FIG. 6. (x,T) phase diagram of $\mathrm{BCC}_{1-x}\mathrm{B}_x\mathrm{D}$ at ambient pressure. The regions of the x-dependent anomalies T_s and T_f are shaded.

and freeze at T_f. If apart from Br some intrinsic pinning centers are considered,[19] $x\approx 0.08$ is equivalent to about 0.6 centers per unit cell. Soliton pinning and the formation of local defects like $\langle 35\rangle_{\mathrm{local}}$ or $\langle 46\rangle_{\mathrm{local}}$ are causes of the dielectric activity of T_s for $E\|b$ in the a polarized $\langle 4\rangle$ and in the nonpolar $\langle 5\rangle$ phase. Thus pinning centers are sources of polarization on a microscopic scale.

(C) This finite $P_{s,b}$, increasing with x, can also be observed via small hysteresis loops in the phases $\langle 4\rangle$ and $\langle 5\rangle$ (Fig. 2). The coercive fields $E_{c,b}$ of these loops change at T_s and T_f as expected (Fig. 7, above): Above T_s, $E_{c,b}$ is close to zero, below it starts to rise with a finite slope, this slope increases at T_f. This behavior is repeated for elevated pressure, when T_s and T_f both shift to higher T, i.e., lines of constant coercive field are parallel to the T_s line and equidistant at low E_c [$E_c\approx\mathrm{const}\cdot(T_s-T)$; Fig. 7, below]. At T_s the coercive field of these loops vanishes, while a small $P_{s,b}$ still exists, but no pinning occurs.

(D) Infrared and Raman spectra taken in the phases $\langle 4\rangle$ and $\langle 5\rangle$ above T_s display diffuse spectra almost identical to

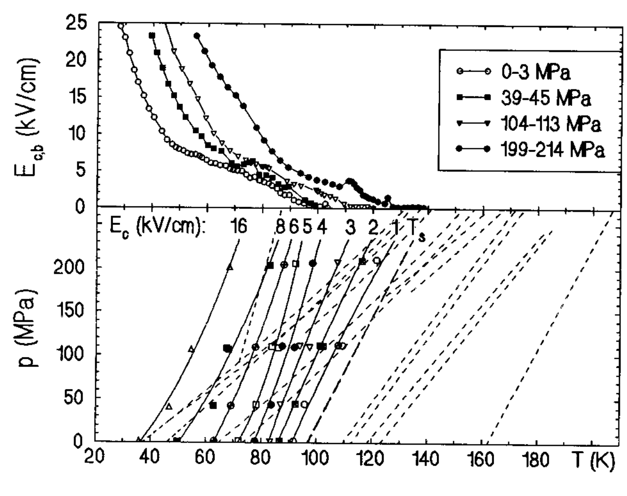

FIG. 7. Above: T dependence of the coercive field $E_{c,b}$ in $\mathrm{BCC_{0.98}B_{0.02}D}$ at various hydrostatic pressures. Below: (p,T) diagram of $\mathrm{BCC_{0.98}B_{0.02}D}$ with the T_s line (broken lines) and lines of constant $E_{c,b}$ (solid lines).

those taken in the ic phase.[13,31] Their fingerprint character used to identify the various c phases below T_s is lost. In a state of gliding harmonic modulation the various molecular units as sources of the specific spectral lines experience varying phases of deformation as in an ic phase. Our results indicate a continuous gliding of an approximately harmonic polarization wave. This result is also supported by theoretical investigations on type-II systems in terms of Landau's theory, e.g., Ref. 32. This mode corresponds to the phason observed in type-I systems near T_i. Different from the situation there, the gliding of the modulation wave in BCCD occurs in an extended temperature range.

(E) Chaves *et al.* have recently performed an elastic neutron-scattering study of partially deuterated BCCD under hydrostatic pressure.[33] They have determined the integrated intensity $I(T,p=\text{const})$ of the satellites in the c and ic phases and observed an increase of this intensity towards lower T. Rather abrupt changes of I are observed on crossing a c-c phase transition. With increasing T for constant pressure, the anomalies for $I(T,p)$ are smoothed, some peaks and plateaus being erased. Finally $I(T,p)$, which is proportional to the squared order parameter, decays linearly with T. If the onsets at low T of these linear ranges of I are located in the (p,T) diagram, again a line parallel to the accumulation line and about 2 K above the T_s line is found. This observation again supports the conclusion that the T_s line and the accumulation line mark constant modulation amplitudes in the (p,T) diagram, and that for $T>T_s$ the modulation in c phases is not basically different from the modulation in the neighboring ic phases and is harmonic.

The very weak frequency dependences of both temperatures T_s and T_f (Fig. 3) result in unphysical Arrhenius and Vogel-Fulcher fit parameters. This indicates that the underlying processes are not of single-particle character, but rather are collective processes in the soliton and the domain-wall regime, respectively, showing strong resemblance to real phase transitions.

V. CONCLUSIONS

The main topics of this work were the analysis of the formation of a soliton system with two sublattices and its field-induced structural phase transitions in the region of an approximately square-wave modulation of the polarization and the collection of experimental data which indicate a state of moving domain walls at elevated T intrinsically pinned to one another. The role of modulation defects becomes apparent. In BCCD the region of the free floating modulation extends from T_i down to T_s, i.e., to the onset of the $\frac{1}{4}$ phase at ambient pressure. At elevated pressure it extends into the $\frac{1}{4}$ or even the $\frac{1}{5}$ phase (Fig. 1). As the symmetries of BCCD in the various c phases depend on the average phase φ of the modulation with respect to the lattice,[34] the T_s anomaly marks a true structural phase transition, from a low-symmetry space group with arbitrary φ above T_s to a state of higher symmetry with fixed φ below T_s. Stated differently, in BCCD for decreasing T, the lock-in transition occurs in two steps: Below T_i the modulation vector $\mathbf{q}$ locks in occasionally at various rational values ($\delta=\frac{2}{7}$, $\frac{3}{11}$, $\frac{4}{15}$ etc.), however it locks into the lattice only below T_s. This result remains to be verified experimentally.

The evolution of the modulation in BCCD is thus remarkably different from what is known from type-I systems and bears for high T some resemblance to the onset of gliding in systems with charge-density waves[3] and in the flux vortices in high-T_c superconductors, where in fact the Ginzburg-Landau functional is also of the ''quadratic-gradient'' type.[4]

ACKNOWLEDGMENTS

We acknowledge financial support from the Deutsche Forschungsgemeinschaft and the Volkswagen-Stiftung.

[1] H. Z. Cummins, Phys. Rep. **185**, 211 (1990).
[2] *Incommensurate Phases in Dielectrics*, edited by R. Blinc and A. P. Levanyuk (North-Holland, Amsterdam, 1986), Vols. 1 and 2.
[3] G. Grüner, Rev. Mod. Phys. **60**, 1129 (1988).
[4] M. V. Feigel'man, V. D. Geshkenbein, A. I. Larkin, and V. M. Vinokur, Phys. Rev. Lett. **63**, 2303 (1989).
[5] P. Bak, Rep. Prog. Phys. **45**, 587 (1982).
[6] W. Selke, Phys. Rep. **170**, 213 (1988).
[7] P. Bak and J. von Boehm, Phys. Rev. B **21**, 5297 (1980).
[8] A. M. Szpilka and M. E. Fisher, Phys. Rev. Lett. **57**, 1044 (1987).
[9] R. Siems and T. Tentrup, Ferroelectrics **98**, 303 (1989).
[10] I. Aramburu, G. Madariaga, and J. M. Pérez-Mato, Phys. Rev. B **49**, 802 (1994).
[11] A. Almeida, M. R. Chaves, J. M. Kiat, J. Schneck, W. Schwarz, J. C. Tolédano, J. L. Ribeiro, A. Klöpperpieper, H. E. Müser, and J. Albers, Phys. Rev. B **45**, 9576 (1992).
[12] O. Hernandez, J. Hlinka, and M. Quilichini, Ferroelectrics **185**, 213 (1996).
[13] G. Schaack, M. le Maire, M. Schmitt-Lewen, M. Illing, A. Lengel, M. Manger, and R. Straub, Ferroelectrics **183**, 205 (1996).
[14] H.-G. Unruh, F. Hero, and V. Dvořák, Solid State Commun. **70**, 403 (1989).
[15] G. Schaack, Ferroelectrics **104**, 107 (1990).
[16] R. Ao, G. Schaack, M. Schmitt, and M. Zöller, Phys. Rev. Lett. **62**, 183 (1989); S. Kruip, G. Schaack, and M. Schmitt-Lewen, *ibid.* **68**, 496 (1992).
[17] M. le Maire, A. López Ayala, G. Schaack, A. Klöpperpieper, and H. Metz, Ferroelectrics **155**, 335 (1994).
[18] M. le Maire, A. Lengel, G. Schaack, and A. Klöpperpieper, Ferroelectrics **185**, 217 (1996).
[19] M. le Maire, *Einfluβ von Gitterdefekten auf die modulierten Phasen von Betain–Calciumchlorid–Dihydrat*, Edition Wissenschaft, Reihe Physik, Vol. 28, Ph.D. thesis, University of Würzburg (Tectum Verlag, Marburg, FRG, 1996).
[20] O. Freitag, H.-G. Unruh, Ferroelectrics **105**, 357 (1990).
[21] A. Klöpperpieper, H. J. Rother, J. Albers, and H. E. Müser, Jpn. J. Appl. Phys. **24**, Suppl. 24-2, 829 (1985).
[22] J. L. Ribeiro, M. R. Chaves, A. Almeida, J. Albers, A. Klöpperpieper, and H. E. Müser, Phys. Rev. B **39**, 12 320 (1989).
[23] P. Neubert, M. Pleimling, T. Tentrup, and R. Siems, Ferroelectrics **155**, 359 (1994).
[24] $\delta=n/m$ with $m=\Sigma_{i=1}^{n}Z_i$ for a structure $\langle Z_1\cdots Z_n\rangle$ (Ref. 23).
[25] J. L. Ribeiro, M. R. Chaves, A. Almeida, H. E. Müser, J. Albers, and A. Klöpperpieper, Phys. Status Solidi B **163**, 511 (1991).

[26] M. Maeda and I. Suzuki, J. Phys. Soc. Jpn. **62**, 1139 (1993).
[27] W. Brill, E. Gmelin, and K. H. Ehses, Ferroelectrics **103**, 25 (1990).
[28] W. L. McMillan, Phys. Rev. B **14**, 1496 (1976); P. Bak and V. J. Emery, Phys. Rev. Lett. **36**, 978 (1976); M. E. Fisher and D. S. Fisher, Phys. Rev. B **25**, 3192 (1982).
[29] J. Bornarel, J. Appl. Phys. **43**, 845 (1972); V. N. Fedosov and A. S. Sidorkin, Sov. Phys. Solid State **19**, 1359 (1977); K. Kuramoto, J. Phys. Soc. Jpn. **56**, 1859 (1987).
[30] M. le Maire G. Schaack, Ferroelectrics **172**, 187 (1995).
[31] M. Illing, G. Schaack, and M. Schmitt-Lewen, Ferroelectrics **155**, 341 (1994).
[32] A. E. Jacobs, Phys. Rev. B **33**, 6340 (1986).
[33] M. R. Chaves, A. Almeida, J. M. Kiat, J. C. Tolédano, J. Schneck, R. Glass, W. Schwarz, J. L. Ribeiro, A. Klöpperpieper, and J. Albers, Phys. Status Solidi B **189**, 97 (1995).
[34] J. M. Pérez-Mato, Solid State Commun. **67**, 1145 (1988).